ChemElectroChem

Review
doi.org/10.1002/celc.202300661

Chemistry Europe
European Chemical Societies Publishing

www.chemelectrochem.org

Emerging Battery Systems with Metal as Active Cathode Material

Kaiming Xue,[a] Huimin Wang,[a] and Denis Y. W. Yu*[a, b]

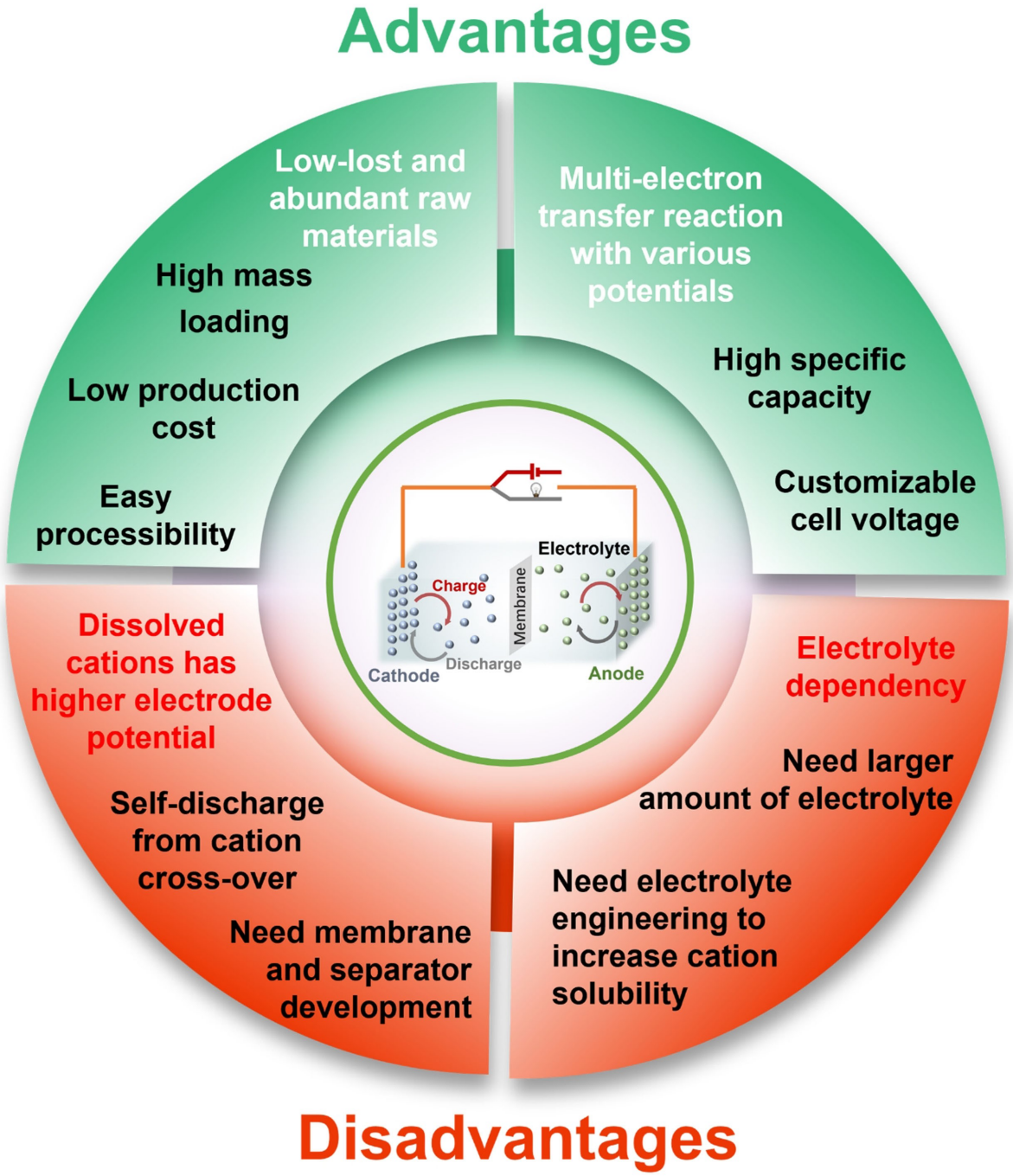

The high-cost and limited availability of raw materials for lithium-ion batteries hinder their future development and urge researchers to explore alternative battery systems. Among them, batteries utilizing the electrochemical redox reaction of metals such as Cu, Fe, Sn, etc. as the cathode to reversibly store and release energy are attractive because their raw materials are common and abundant. This review examines this type of novel battery system, introduces its basic mechanism and problems, analyses the strategies that are used to improve its reversibility and cycling stability and also proposes some possible future directions of investigations.

1. Introduction

As an important device to reversibly store and release electrical energy, battery has become an indispensable part of our daily life to power consumer electronics such as cell phones, laptops, cameras and supplement the electricity grid.[1,2] Especially, the fast advancement of electrical vehicles in this decade further fosters the growth of the battery industry.[3] However, lithium-ion battery (LIB), one of the most common battery systems, faces an obstacle for large-scale applications because of its high cost caused by limited reserves of its raw materials.[4] Due to the utilization of lithium, whose price has witnessed a constant increase in recent years, and other expensive transitional metal elements such as Ni and Co, the active cathode materials account for the largest portion (about 30%) of the raw materials cost for the battery.[5]

In this respect, other novel battery systems using alternative cathodes are being intensively investigated by the research community.[6–11] For example, lithium-O_2 (Li–O_2)[6] and lithium-sulfur (Li–S)[7] batteries that use inexpensive carbon electrode as host for O_2 and sulfur electrode, respectively, as the cathodes are potential low-cost systems. Recently, the use of common metals as electrodes is also attracting more and more interest from researchers. Metals such as Li, Al, and Sn are frequently investigated as the battery anode in organic electrolytes, whereas Zn and Fe are studied as anode with aqueous electrolytes.[12–14] In comparison, the use of metal as active cathode materials is still in its infancy. Therefore, a review of novel battery systems using metal cathodes would be timely and helpful for the advancement of these unconventional battery systems. In this review, we systematically summarized various kinds of metal cathodes from copper, which is the most commonly used metal cathode because of its low price and high redox potential, to other metals ranging from silver and stainless steel to tin and other Group IV, V, and VI metals. The performances of these batteries are demonstrated in different types of electrolytes, such as aqueous-based electrolyte, organic-based electrolyte, aqueous/organic mixed electrolyte, and molten salt electrolyte. Such variability allows the potential utilization of metal cathodes in a wide spectrum of electrochemical energy storage applications.

In general, metals can undergo redox reactions at a certain potential and reversibly convert between metal atoms and metal cations by giving out electrons during charging and accepting electrons during discharging to store and release electrical energy, as demonstrated in the following reactions:

$$charge: M - ne^- \rightarrow M^{n+}$$

$$discharge: M^{n+} + ne^- \rightarrow M$$

Since different metals have different electrode potentials, as shown in Table 1, the output voltage of the resulting battery systems using metal as active cathode materials is determined by the electrode potential difference between the cathode and the anode. For example, since the electrode potential of Sn/Sn^{2+} and Li/Li^+ is −0.13 and −3.04 V (relative to a standard hydrogen electrode), respectively, the working voltage of the corresponding Sn–Li battery with Sn cathode and Li anode is about 2.8 V (the actual value may vary slightly from the theoretical value due to different electrolytes).

The advantages of metals are that they have excellent electrical conductivity and often have high specific capacity as multiple electrons can be extracted.[15] They also have good processibility so that the direct utilization of metal foils as electrodes is possible. So, when preparing the electrode, polymer binders, conductive additives, and toxic organic solvents are not necessary, which simplifies the manufacturing process and increases the loading amount of active cathode materials. If metal powder is used, they can still be slurry-coated

Table 1. Standard potentials of different metals.

Half reaction	Standard Potential (V)
$Ag^+ + e^- \Leftrightarrow Ag$	+0.80
$Cu^{2+} + 2e^- \Leftrightarrow Cu$	+0.34
$2H^+ + 2e^- \Leftrightarrow H_2$	0
$Sn^{2+} + 2e^- \Leftrightarrow Sn$	−0.13
$Ni^{2+} + 2e^- \Leftrightarrow vNi$	−0.25
$Fe^{2+} + 2e^- \Leftrightarrow Fe$	−0.44
$Zn^{2+} + 2e^- \Leftrightarrow Zn$	−0.76
$Ti^{3+} + 3e^- \Leftrightarrow Ti$	−1.37
$Na^+ + e^- \Leftrightarrow Na$	−2.71
$Li^+ + e^- \Leftrightarrow Li$	−3.04

[a] Dr. K. Xue, Dr. H. Wang, Prof. D. Y. W. Yu
School of Energy and Environment, City University of Hong Kong Kowloon, Hong Kong, China
E-mail: yu.denis@nims.go.jp
Homepage: https://samurai.nims.go.jp/profiles/yu_denis?locale=en
[b] Prof. D. Y. W. Yu
Research Center for Energy and Environmental Materials (GREEN), National Institute for Materials Science, 305-0044 Tsukuba, Ibaraki, Japan

in the same way as traditional LIB electrodes. In this review, the specific capacity and current density are expressed in mAh cm^{-2} and mA cm^{-2} for metal foil electrodes or mAh g^{-1} and mA g^{-1} for metal powder electrodes.

The main issue of using metal as the cathode material in a battery is that of the self-discharge caused by the shuttling of cathode metal cations that are generated in the charge process from the catholyte to the anolyte, which are spontaneously reduced at the anode. This will lead to low Coulombic efficiency (CE), large energy loss, and poor cycling stability. In addition, the cathode materials will be continuously consumed, causing the gradual disintegration of the electrode. Moreover, the anode will be poisoned by the "alien" cathode material, affecting the deposition process of the anode material. Strategies to overcome the shuttling problem mainly target at regulating and modifying the separator and electrolyte, which will be illustrated in detail in this review.

2. Copper Cathode

Copper has both advantages of low cost and high redox reaction potential over common metals. In addition, it is stable in both aqueous and organic electrolytes. Therefore, most investigations to date utilize copper as the active cathode materials.

2.1. Cu-BasedBattery Coupled with low Electrode Potential Anodes such as Li and Al–Li SIloy

2.1.1. Charge-Discharge mechanism

When a Cu-based cathode is coupled with a low electrode potential anode such as Li and Al–Li alloy, the corresponding battery will have an output voltage of about 3 V. Though, organic electrolytes with larger electrochemical window will have to be used in these batteries to keep the anode stable. Huang et al. first demonstrated the feasibility of a coin cell with Cu and Li foils as the cathode and anode, respectively, with a carbon-coated polypropylene (PP) separator in an electrolyte of 1.0 M $LiClO_4$ in ethylene carbonate (EC) : propylene carbonate (PC) = 1 : 1 (volume ratio).[16] The voltage profiles of the battery are shown in Figure 1a. They attributed the oxidation process to a one-step reaction from Cu to Cu^{2+} whereas the reduction process is a two-step reaction first from Cu^{2+} to Cu^{+} and then to Cu from the incremental charge versus potential (dQ/dV) curve (Figure 1b). Though, their obtained areal capacity is only about 0.014 mAh cm^{-2}.

In 2019, Wang and Yu proposed that Cu undergoes a one-electron transfer to Cu^{+} in a lithium bis(trifluoromethanesulfonyl)imide (LiTFSI)/dimethyl carbonate (DMC)-based organic electrolyte during charging if the charge capacity is limited.[17] They verified it by quantifying the amount of Cu cations in the electrolyte solution at different states of charge with inductively coupled plasma mass spectroscopy (ICP-MS) and comparing the experimental value with the theoretical amount of Cu^{+}, as shown in Figure 1c.

It is worthy to note that the mechanism of Cu cathode is still controversial and perplexing as the stability of different cations (Cu^{+} or Cu^{2+}) may depends on the choice of electrolyte, i.e. lithium salts (e.g. $LiClO_4$ vs. LiTFSI) and solvents (e.g. EC/PC vs. DMC). A systematic investigation in the future is necessary to obtain a thorough understanding of the reaction mechanism of Cu cathode in organic electrolytes.

2.1.2. Suppression of the Cross-Over of Cu Cations

Though, if the Cu ions from the catholyte cross-over to the anolyte, the CE of the battery will be decreased because the Cu ions can be readily reduced at the anode, which poses a large

Dr. Kaiming Xue received his bachelor degree from Zhejiang University in 2019. In 2023, he obtained his Ph.D. degree from City University of Hong Kong under the supervision of Dr. Denis Yu. His research interest focuses on the separator modification and electrolyte design for different metal-cathode batteries.

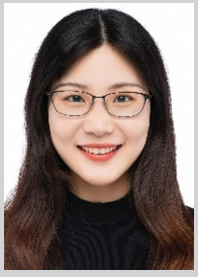

Dr. Huimin Wang is a researcher specializing in the field of energy storage, specifically in the area of metal cathodes, electrolyte design and novel battery systems. She obtained her bachelor's degree from Anhui University and successfully completed her Ph.D. studies in 2020 at City University of Hong Kong, under the guidance of Dr. Denis Y.W. Yu.

Prof. Denis Yu is the group leader of the Rechargeable Battery Materials Group at the National Institute for Materials Science in Japan. He received his bachelor's degree from Princeton University and his Ph.D. degree from Harvard University. His research interest includes understanding fundamental reaction mechanisms in battery materials and electrodes, centering on examining the effect of surface chemistry and structure on electrochemical performances, as well as on the long-term stability and safety of batteries.

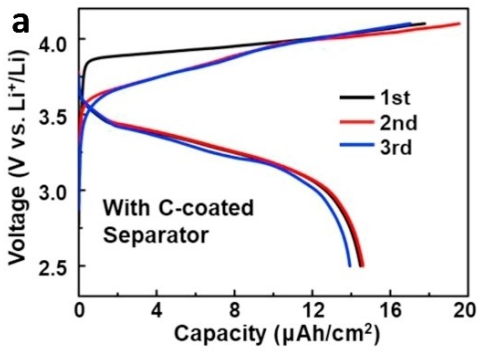

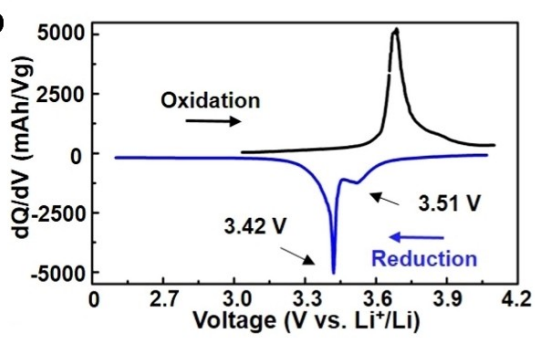

c

state	cumulative capacity (mAh)	measured Cu content (ppm)	estimated M^+ in electrolyte (ppm)
as-purchased electrolyte	0	0	0
(A) charged for 5 h	0.225	7.21	8.40
(B) charged for 10 h	0.45	14.02	16.80
(C) charged for 10 h, followed by discharge to 2 V	0.27	5.92	6.72

[a]Cu contents obtained from ICP-MS in electrolyte of Cu–Li cells at different states of charge.

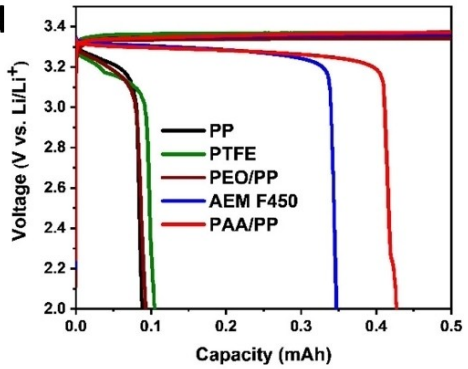

Figure 1. (a) Charge-discharge curves of Cu/Li coin cell with a C-coated Celgard separator; (b) the incremental charge versus potential (dQ/dV) curve of Cu@CNFs electrode during the charge/discharge process (re-print with permission from [16] Copyright 2018, Elsevier); (c) variation of Cu contents in electrolyte (re-print with permission from [17] Copyright 2019, American Chemical Society); (d) fifth cycle charge–discharge curves at a current density of 0.01 mA cm^{-2} for Cu–Li batteries with different separators (re-print with permission from [19] Copyright 2021, American Chemical Society).

problem to the reversibility of the battery. Conventional separators commonly used in LIBs such as polypropylene (PP) membranes have high porosity, but they are not ion-selective, which means any ions (cations and anions) can freely pass through them.[18] Figure 1d shows the voltage profiles of a Cu–Li with PP membrane in 3 M LiTFSI in DMC electrolyte at a current rate of 0.01 mA cm^{-2}.[19] The CE of the battery is extremely low because of the cross-over of Cu ions. Techniques to suppress the cross-over of Cu ions are necessary to improve the reversibility of the battery with the Cu cathode. So far, the strategies that are demonstrated are shown in Figure 2, by (a) tuning the interaction between the electrolyte and separator, (b) addition of the Cu trapping layer, (c) use of anion exchange membrane, and (d) use of a ceramic separator.

2.1.2.1. Interaction Between Electrolyte and Separator

Wang et al. have found that the migration of Cu ions through PP (Celgard 2400) membrane in fact depends on the type of electrolyte and its interaction with the membrane.[20] As shown in Figure 3a, by screening different kinds of solvents commonly used for battery electrolytes, they found that the Cu–Al battery with 3 M LiTFSI in fluoroethylene carbonate (FEC) electrolyte displays the highest CE. They also noted that there is a correlation between the CE of the battery and the contact angle of the electrolyte on the PP membrane, with higher contact angle giving higher CE. Since the contact angle reflects the surface energy between the electrolyte and the separator, these results suggest that the high surface energy between the PP membrane and the electrolyte suppresses the disadvantageous shuttling of Cu ions across the PP separator. However, the FEC electrolyte shows poorer wetting compatibility with the PP membrane, leading to a larger cell resistance and limiting the rate performance of the battery. Nonetheless, the work demonstrated that the interaction between the electrolyte and membrane can significantly influence the ion transport through the membrane, which is an area that needs further investigation for batteries with metal cathode.

2.1.2.2. Trapping of Cu

To stop the Cu cations from moving from the catholyte to the anolyte, another method is to add a coating layer that can trap the Cu cations on the electrode or the separator to prevent them from moving across to the anode.

Wang et al. first coated the Cu cathode with a layer of polyacrylonitrile (PAN), which improves the CE of the corresponding Cu–Al battery. The PAN polymer has a large amount of electron-rich nitrile (–C–N) groups in its molecular structure, which is a Lewis base and is able to interact with Cu^+ (Lewis

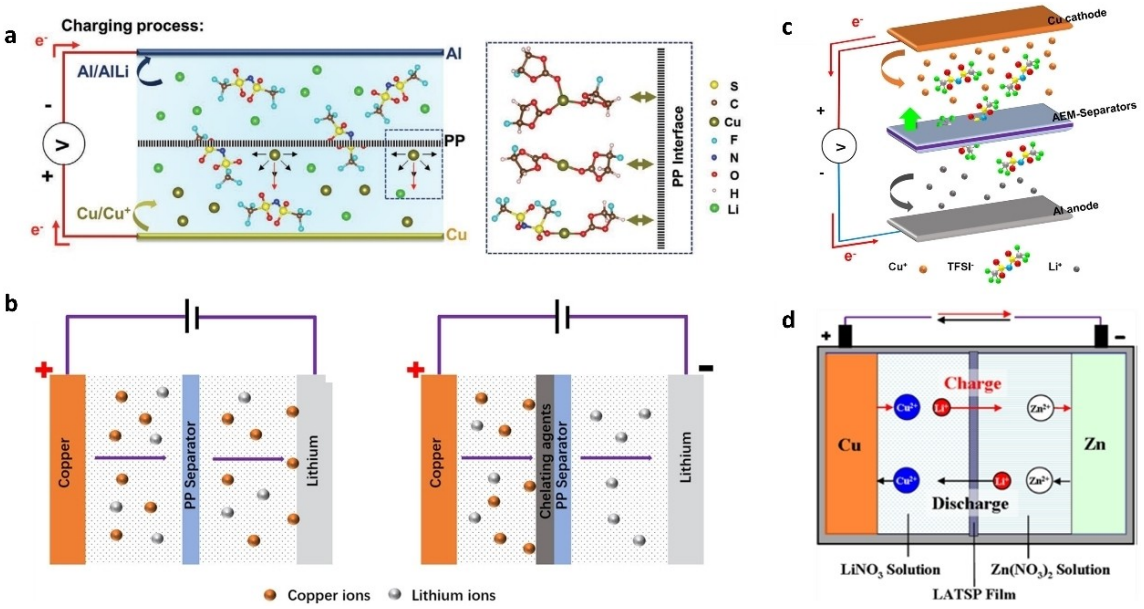

Figure 2. Strategies to solve the cross-over problem: (a) tuning the interaction between the electrolyte and separator (re-print with permission from [20] Copyright 2020, Wiley-VCH); (b) addition of the Cu trapping layer (re-print with permission from [19] Copyright 2021, American Chemical Society); (c) use of anion exchange membrane (re-print with permission from [17] Copyright 2019, American Chemical Society) and (d) use of a ceramic separator (re-print with permission from [21] Copyright 2014, Springer Nature).

acid) in the electrolyte solution to anchor the Cu^+ ions and prevent them from passing through the electrolyte and participating in possible side reactions with the anode.[22] As shown in Figure 3b and 3c, the CE of the Cu–Al battery with the PP membrane tested in the 3 M LiTFSI FEC electrolyte at a current rate of 0.014 mA cm^{-2} can be increased from about 92% to 98% after the introduction of the PAN layer. Although the PAN polymer coated on the cathode surface may help immobilize Cu^+, the intactness of the PAN layer in the cycling process is questionable since it may be detached from the cathode surface along with the dissolution of Cu during the charging process.

Besides coating on the electrode, in another work, Xue et al. coated the commercial PP separator with polyacrylic acid (PAA), a chelating polymer, to fabricate a composite membrane of PAA/PP to confine the shuttling of Cu^+ through the modified membranes (Figure 2b).[19] By utilizing the chelating interaction between the carboxyl groups in the polymer and copper ions, the chelating polymer can prevent the movement of Cu^+ from the catholyte to the anolyte in the cell and suppress the self-discharge of the corresponding battery. The Cu–Li battery with the PAA/PP membrane (86%) shows much higher CE than the one with the pristine PP separator (20%) and commercial anion exchange membrane (AEM) (70%) at a rate of 0.01 mA cm^{-2}, as shown in Figure 1d. By contrast, other polymer coatings such as polyethylene oxide (PEO) show low CE as they do not contain the same carboxyl groups as the PAA polymer that can trap the Cu cations.

Though, the physical coating of a PP separator with functional polymers can produce other problems, such as the increase in the resistance of the battery. In Xue et al.'s work, although the PAA/PP membrane improves the reversibility, the battery exhibits unsatisfactory rate performance whose average discharge voltage drops significantly from 3.08 V at 0.1 mA cm^{-2} to 2.07 V at 1 mA cm^{-2} as the PAA layer limits the transport of other ions besides Cu^+ through the membrane as well (Figure 3d), especially at increased current rates.[19] To reduce the voltage polarization, the authors introduced barium titanate (BTO) nanoparticles into the PAA/PP membrane, which is shown to enhance the ionic transfer through the membrane and increase the average discharge voltage to 2.85 V at 1 mA cm^{-2}.

Since Cu cations are being trapped into the polymer layer, one of the other concerns is whether the effect of these polymer coating can be long-lasting as the Cu cations will accumulate inside the polymer with cycling, and eventually saturating the layer. Further work is necessary to study how the ion blocking capability of the polymers is influenced by the accumulation of Cu ions. In addition, efficient ion transport channels through the trapping layer need to be constructed to keep the resistance of the battery low.

2.1.2.3. Use of Anion Exchange Membrane (AEM)

With the new developments in ions-selective membranes, it is now possible to tune the type of ions that are transported through them. So, in principle, the cross-over of Cu cations can be stopped with the use of an AEM, in which the charge balance within the battery will be maintained by the transport of anions.

Wang et al. demonstrated that the use of a commercially-available anion exchange membrane (AEM – FAPQ-310-PP (F310)) as the separator can improve the CE of a Cu–Al battery.[17] Interestingly, the effectiveness of the F310 mem-

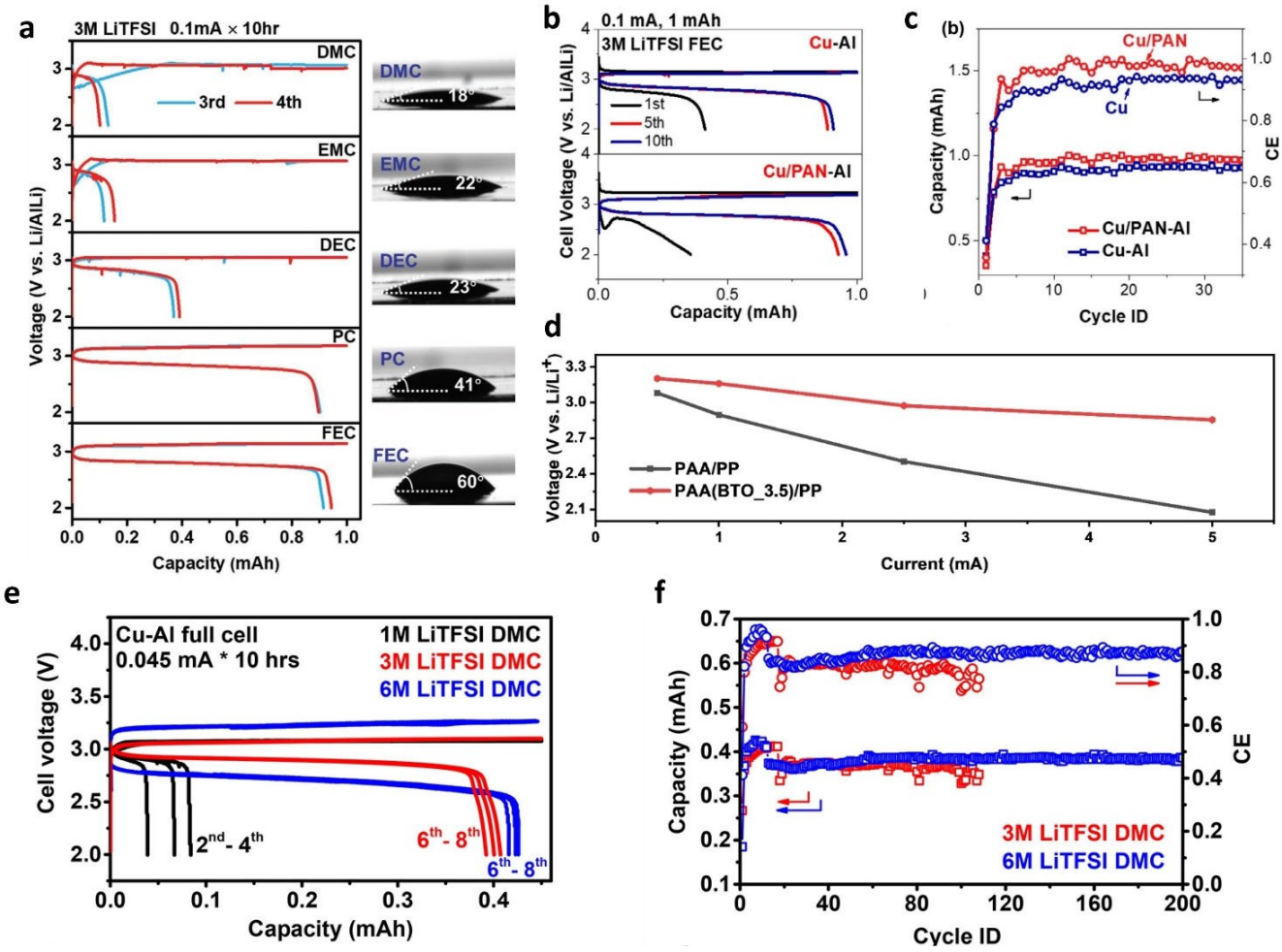

Figure 3. (a) Voltage profiles of Cu–Al batteries with a PP membrane at a constant rate of 0.014 mA cm^{-2} and a capacity limit of 0.14 mAh cm^{-2} in 3 M LiTFSI in DMC, EMC, DEC, PC, and FEC; photographs showing the contact angles (CA) of 3 M LiTFSI DMC, EMC, DEC, PC, and FEC electrolytes on a PP membrane at room temperature (re-print with permission from [20] Copyright 2020, Wiley-VCH); (b) charge/discharge curves of a Cu–Al cell and a Cu/PAN–Al cell in 3 M LiTFSI FEC at a current density of 0.014 mA cm^{-2} and a capacity limit of 0.14 mAh cm^{-2}; (c) cycle performances of the Cu–Al and Cu/PAN–Al cells; and electrochemical performance of Cu–Al full cell (re-print with permission from [22] Copyright 2021, Elsevier); (d) average discharge voltage of Cu–Li batteries at different current rates with different separators (re-print with permission from [19] Copyright 2021, American Chemical Society); (e) voltage profiles and (f) cycle performance of Cu–Al full cells at a rate of 0.0225 mA cm^{-2} and a capacity limitation of 0.225 mAh cm^{-2} in 1, 3, and 6 M LiTFSI DMC electrolytes, respectively, (re-print with permission from [17] Copyright 2019, American Chemical Society).

brane depends on the concentration of the electrolyte. Specifically, CE is 19%, 80%, and 88% at a rate of 0.0225 mA cm^{-2} with an areal capacity limitation of 0.225 mAh cm^{-2} for cells tested in 1 M, 3 M, and 6 M electrolyte with LiTFSI and DMC, respectively and the cycle performance is better with higher salt concentrations (Figure 3e and 3f). The improvement is ascribed to the different solvation structures within the electrolyte. With the increase in the salt concentration, the Cu ions are most likely incorporated into large solvation structures such as contact ion pairs (CIP) and aggregate (AGG), which are harder to cross through the AEM. However, the increased interaction between the salt and the solvent molecules also limits the transfer of anions through the AEM, resulting in higher overpotential (Figure 3e). This work demonstrates that the synergistic effect of a AEM membrane, which only conducts anion but blocks cations, with a highly concentrated electrolyte can reduce the shuttling of Cu^+ and increase the CE of the battery.

Though, commercial AEMs are typically developed for the use in the aqueous medium with counter anions such as SO_4^{2-} or Cl^-, which may not be directly suitable for Cu-based battery in the organic-based aprotic electrolyte.[23] In view of this, Xue et al. designed a membrane with a poly(ionic liquid) (PIL) of poly(diallyldimethylammonium bis(trifluoromethylsulfonyl)imide) ($PDADMA^+TFSI^-$) coated on a commercial PP separator (PIL/PP) that can be used in organic electrolytes.[24] The PIL contains a positively-charged polymer backbone with $TFSI^-$ anions, with a molecular structure as shown in Figure 4a, which can block the shuttling of copper ions via an electrostatic repulsion effect. It is also compatible with the LiTFSI salt typically used in electrolytes for Cu-based batteries.

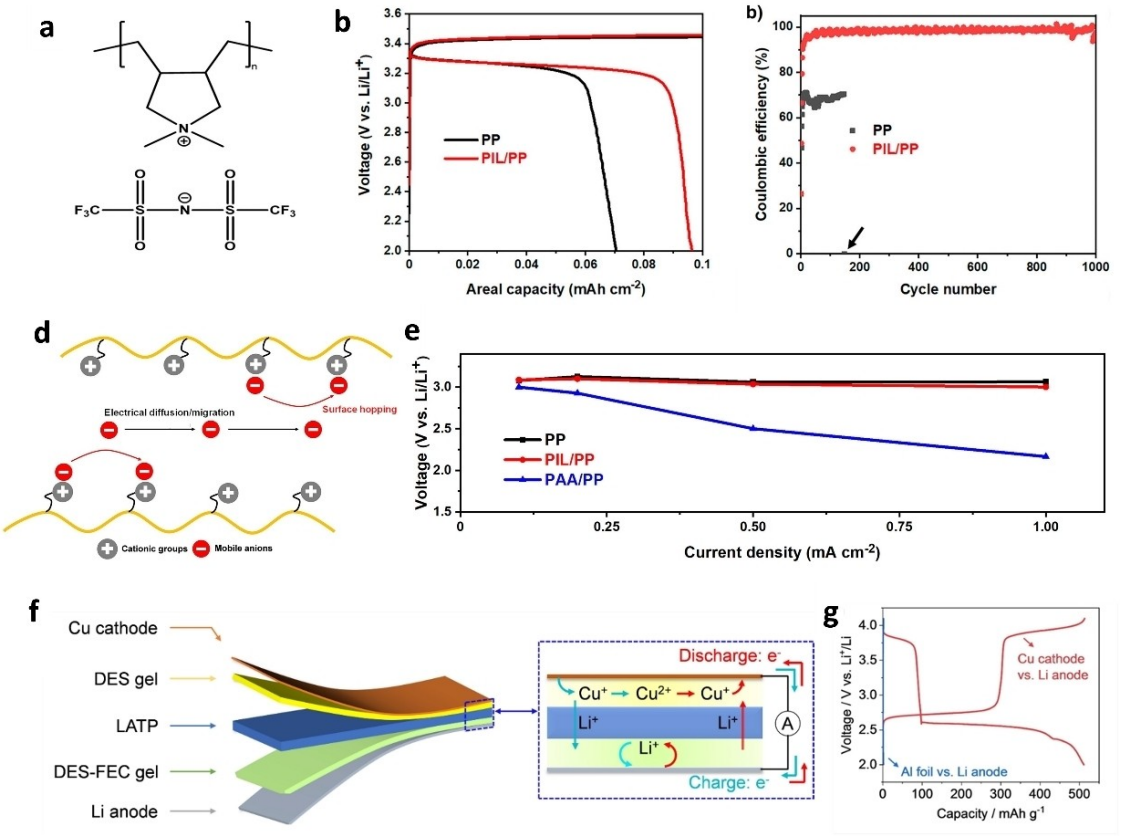

Figure 4. (a) Molecular structure of PDADMA-TFSI; (b) The 20th cycle charge–discharge curves and (c) cycle performances of Cu–Li batteries at a rate of 0.2 mA cm^{-2} with different separators; (d) schematic diagram of the anion transport mechanism through the PIL polymer; (e) average discharge voltage of Cu–Li batteries with the PIL/PP membrane at different current rates (re-print with permission from [24] Copyright 2023, Wiley-VCH); (f) schematic diagram of a solid-state Cu–Li battery with a Cu cathode, a Li anode, and a multilayer electrolyte consisting of DES gel, LATP pellet, and DES-FEC gel; (g) charge-discharge curves of the solid-state Cu–Li battery at a rate of 200 mA g^{-1} between 2–4.1 V. (re-print with permission from [15] Copyright 2022, Wiley-VCH)

Specifically, the PIL is first dissolved in N-methyl-2-pyrrolidone (NMP) solvent and coated on a commercial PP separator to make a PIL/PP membrane for easy handling. Xue et al. then constructed a reversible 3.3 V Cu–Li battery in 3 M LiTFSI DMC electrolyte with the membrane.[24] The battery demonstrated superior reversibility and cycling stability with CE of 99% for over 1000 cycles (Figure 4b and 4c) at the current rate of 0.2 mA cm^{-2} and capacity limit of 0.1 mAh cm^{-2}. In addition, since the positively charged polymer backbone can provide additional channels to transport anions (Figure 4d), the battery shows fast kinetics and reduced voltage polarization, with only a 0.15 V drop in discharge voltage when the current rate is incremented from 0.1 mA cm^{-2} to 1 mA cm^{-2} (Figure 4e).

2.1.2.4. Use of a Ceramic Separator

Apart from ion-selective membranes, there are also solid-state conductors that can allow selective transport of a certain type of ions. For example, $Li_{1+x}Al_xTi_{2-x}(PO_4)_3$ (LATP) ceramic is a type of sodium super ionic conductor (NASICON) solid electrolyte that allows the transfer of Li^+ but not other cations. So, it is possible to use a ceramic separator to prevent the cross-over of Cu ions.

For example, Wang et al. tested a Cu–Li battery with a sandwiched solid-state electrolyte of DES gel/LATP/DES-FEC gel. The deep-eutectic-solvent-based gel (DES gel) was prepared by mixing a DES solution composed of LiTFSI and succinonitrile (SCN) with ethoxylated trimethylolpropane triacrylate (ETPTA) monomer and 1 wt% azobisisobutyronitrile (AIBN) initiator and polymerizing it at 70 °C (Figure 4f). The $Li_{1.4}Al_{0.4}Ti_{1.6}(PO_4)_3$ (LATP) interlayer can help inhibit the passing through of copper cations. The Cu powder cathode of the Cu–Li battery can exhibit a specific capacity as high as 500 mAh g^{-1} (Figure 4g). This work inspires future application of solid-state electrolytes in batteries with metal cathodes.

Because a ceramic is non-porous, it also allows the use of two different electrolytes, an aqueous electrolyte on the Cu cathode side with an organic electrolyte on the Li anode side. Wang et al. has demonstrated such a battery with 2 M $LiNO_3$ (aq) electrolyte for the Cu cathode and 1 M $LiClO_4$ in EC/DMC electrolyte for the lithium anode using a LISICON film (Figure 5a).[25] As shown in Figure 5b, the Cu–Li battery with such configuration can achieve a discharge voltage about 3 V. Besides Cu, Ag and Ni were also studied in such an organic/aqueous hybrid electrolyte and exhibit specific capacity of about 250 mAh g^{-1} and 640 mAh g^{-1}, respectively.[26] Though, one of the drawbacks of this configuration is the potential risk

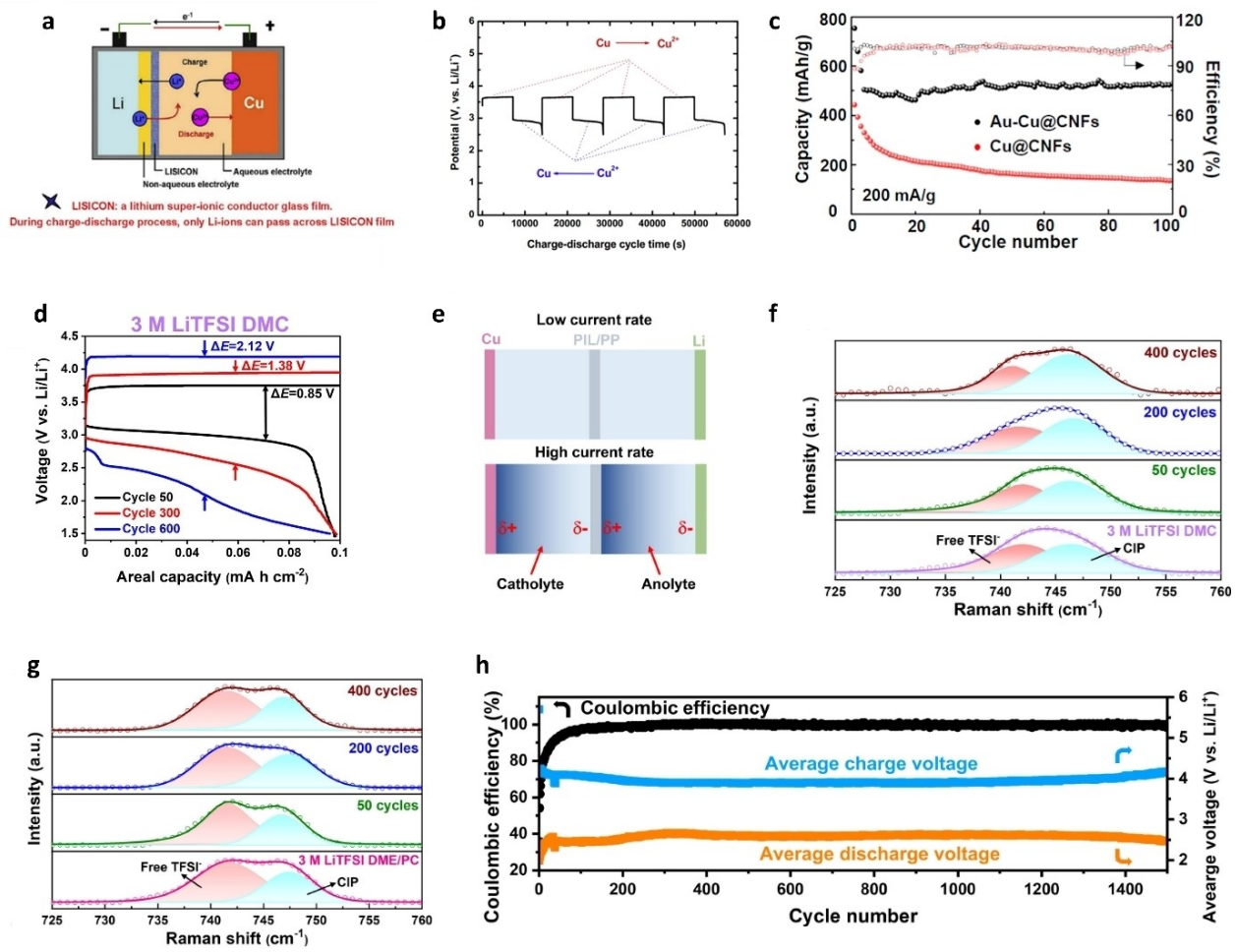

Figure 5. (a) Schematic diagram and operating principles of a Cu–Li battery with solid-state separator; (b) cycle performance of the Cu–Li battery: continuous charge–discharge curve (re-print with permission from [25] Copyright 2009, Elsevier); (c) cycling performance of Cu@CNFs and Au–Cu@CNFs electrodes at 200 mA g^{-1} (re-print with permission from [16] Copyright 2018, Elsevier); (d) selected voltage profiles of a Cu–Li battery tested in 3 M LiTFSI DMC with PIL/PP membrane; (e) proposed concentration gradient in the battery with the 3 M LiTFSI DMC electrolyte; Raman spectra of (f) 3 M LiTFSI DMC and (g) 3 M LiTFSI DME/PC = 3 : 7 electrolytes extracted from cycled Cu–Li batteries; (h) cycle performance of the Cu–Li battery with 3 M LiTFSI DME/PC electrolyte at 2 mA cm^{-2} (re-print with permission from [27] Copyright 2023, Elsevier).

of electrolyte leakage. In the event that the aqueous electrolyte seeps into the anode side, the Li anode will react violently with water, potentially causing a fire.

2.1.3. Other Factors Affecting Cycle Stability

Cross-over of Cu cations through the membrane is one of the factors affecting the cycle stability of the batteries with the Cu cathode. In addition, the uniformity of the stripping and deposition of Cu on the cathode and the change in the solvation structure of the electrolyte with cycling will also affect the cycling performance of the cathode.

Huang et al. made a composite cathode with a network of Cu nanoparticles and carbon nanofibers (Cu@CNFs) that showed a specific discharge capacity of 635 mAh g^{-1} in the first cycle but with fast capacity fading with cycling.[16] They attributed the capacity lost to the aggregation of re-deposited Cu. By coating the composite cathode with Au nanoparticles, which can provide nucleation sites for Cu deposition, they demonstrated improved discharge capacity and cycle stability, as shown in Figure 5c.

In general, uneven stripping and deposition of Cu during charge and discharge will cause the formation and growth of pits, islands, and dendrites, which will eventually lead to the disintegration of the electrode. Therefore, to improve the stability of Cu cathodes, methods such as electrode coating or electrode additives will have to be explored in the future.

In addition to the electrode, the status of the electrolyte and its interaction with the membrane while cycling can also affect the reversibility of the battery with Cu cathode. For example, even though the use of a PIL/PP membrane can enable a high CE, Xue et al. showed that the Cu–Li battery with DMC-based electrolyte gives inferior and gradually deteriorating dynamical performance at a higher current rate of 1 mA cm^{-2} (Figure 5d). They attributed it to the buildup of a concentration gradient upon charge-discharge at the high current rate in the presence of the PIL/PP membrane, which only conducts anions

(Figure 5e).[27] Besides, the accumulation of Cu^+ in the electrolyte changes its solvation structure, causing the formation of more CIP in the electrolyte and reducing the amount of free anions in the electrolyte (Figure 5f), resulting in higher resistance for $TFSI^-$ transport through the PIL/PP membrane and increasing the voltage polarization of the Cu–Li battery with cycling. The authors found that the solvation structure of the electrolyte and the interaction of it with the membrane differ with different electrolyte. They then designed a novel mixed solvent with dimethoxyethane (DME) and propylene carbonate (PC) to replace the original DMC solvent, which shows higher ionic conductivity with more free $TFSI^-$ anions that reduces the resistance of ion transport both in the electrolyte and through the membrane. In addition, the electrolyte can help keep a stable solvation structure upon cycling (Figure 5g). These advantages of the new DME/PC based-electrolyte help the Cu–Li battery to cycle stably for more than 1500 cycles at a rate of 2 mA cm^{-2} (Figure 5h).

Unlike LIBs, where the overall composition of the electrolyte remains unchanged during charge and discharge due to a rocking chair mechanism, that of the electrolyte in batteries with metal cathodes involving the dissolution and deposition of metal cations will change within a cycle, and possibly upon cycling as well due to side reactions. Thus, further characterizations and analyses are needed to understand how the interaction between the electrolyte and membrane and the transport mechanism of ions inside the cell change with cycling and affect the performances of the battery.

2.2. Cu-Based Battery Coupled with High Electrode Potential Anode such as Zn

The use of copper as the cathode and Zn as the anode in an aqueous battery dated back to 1836, when the Daniell cell was invented by John Frederic Daniell, a UK chemist. The Daniell cell has two separate electrolytes of $CuSO_4$ solution and $ZnSO_4$ solution for the Cu cathode and Zn anode, respectively. They are connected by a salt bridge, which serves to maintain the charge balance and complete the internal circuit during operation. The battery functions on the basis of the electrochemical reduction reaction on the Cu cathode of $Cu^{2+} + 2e^- \rightarrow Cu$ and electrochemical oxidation reaction on the anode of $Zn - 2e^- \rightarrow Zn^{2+}$ with an overall voltage of about 1.1 V. The Daniell cell is a primary battery, which cannot be recharged due to the severe cross-over of the Cu cations in the catholyte to the anode, a similar problem as described in the Cu–Li battery with organic electrolyte.

There are some recent works on improving the reversibility of Cu–Zn battery to make it rechargeable. For example, Dong et al. utilize a thin ceramic film made of lithium super-ionic conductor (LATSP, $Li_{1+x+y}Al_xTi_{2-x}Si_yP_{3-y}O_{12}$) as the separator of the Cu–Zn battery and two distinct electrolytes of 2 M $LiNO_3$ and 1 M $Zn(NO_3)_2$ solutions as the catholyte and anolyte, respectively.[21] The LATSP allows the transfer of Li and blocks the cross-over of Cu cations. Figure 2d displays a schematic diagram of the working mechanism and assembly, while a photo of the battery is shown in Figure 6a. The reported battery can be normally charged and discharged for about 150 cycles (Figure 6b). Even though the CE is improved, the Cu–Zn battery exhibits high polarization voltage (voltage difference between charge/discharge voltages) of about 0.5 V at a current rate of 0.25 mA cm^{-2} probably due to high resistance of the LATSP ceramic. The LATSP ceramic film is also brittle, which is vulnerable to breaking during the battery assembly and operation.

Similarly, Zhang et al. used a composite separator of PVDF/PMMA–$LiClO_4$/PVDF and two electrolytes of 0.1 M $CuSO_4$/1 M Li_2SO_4 and 0.1 M $ZnSO_4$/1 M Li_2SO_4 for the cathode and anode cells, respectively.[28] The schematic diagram of the working mechanism and photo of the corresponding H-cell are exhibited in Figure 6c and 6d, respectively. However, the cell needs a complex composite separator with two different electrolytes, which restricts the form of the battery to an H-cell. New cell design is needed to make it more suitable for practical use.

Jameson et al. further adopted a CIMS membrane (ASTOM company) as the separator and used 1 M $ZnSO_4$ solution as anolyte and 0.1 M $CuSO_4$/1 M Na_2SO_4 mixed solution as catholyte.[29] CIMS is a specially designed monovalent cation exchange membrane which allows the conduction of monovalent cations and block divalent cations. The membrane therefore permits the shuttling of Na^+ between the cathode side and anode side to maintain the charge balance (Figure 6e). They used 3D printing to fabricate two identical parts to assemble the Cu–Zn battery, which can be cycled for about 100 cycles (one component is shown in Figure 6f). Though, they only demonstrated a cell with cycling stability of up to 100 cycles with an average CE of about 70% and polarization voltage of about 0.35 V at 0.5 mA cm^{-2} (Figure 6g), so more work is needed to study its long-term cycle stability.

Similarly, the use of an AEM is another possible method to suppress the Cu ion cross-over in the aqueous electrolyte. For example, He et al. demonstrated an ampere-hour level Cu–Zn pouch cell with the use of an AEM to enhance the CE of the battery (Figure 6h).[30] For the catholyte side, they used an electrolyte with 1 M $CuSO_4$ (pH = 1) to improve the reversibility of the Cu stripping/plating processes. On the other side, they stabilized the dissolution/deposition of Zn in a $ZnSO_4$ electrolyte by coating it with a 1 μm thick Sn layer.

Alternatively, instead of utilizing a membrane or ceramic to separate the catholyte and anolyte, Zhu et al. demonstrated a concept to use an alkaline-based electrolyte of 1 M KOH solution for both cathode and anode to limit the solubility of Cu^{2+} (Figure 6i).[31] Specifically, Cu will become insoluble Cu-$(OH)_2$ and CuO in the alkaline medium during the charge process and the Cu metal is recovered during the discharge process. The reactions are shown below:

$$\text{Cathode}: \quad Cu(OH)_2/CuO + 2e^- \leftrightarrow Cu$$

$$\text{Anode}: \quad Zn - 2e^- \leftrightarrow Zn(OH)_2/ZnO$$

$$\text{Overall}: \quad Cu(OH)_2/CuO + Zn \leftrightarrow Cu + Zn(OH)_2/ZnO.$$

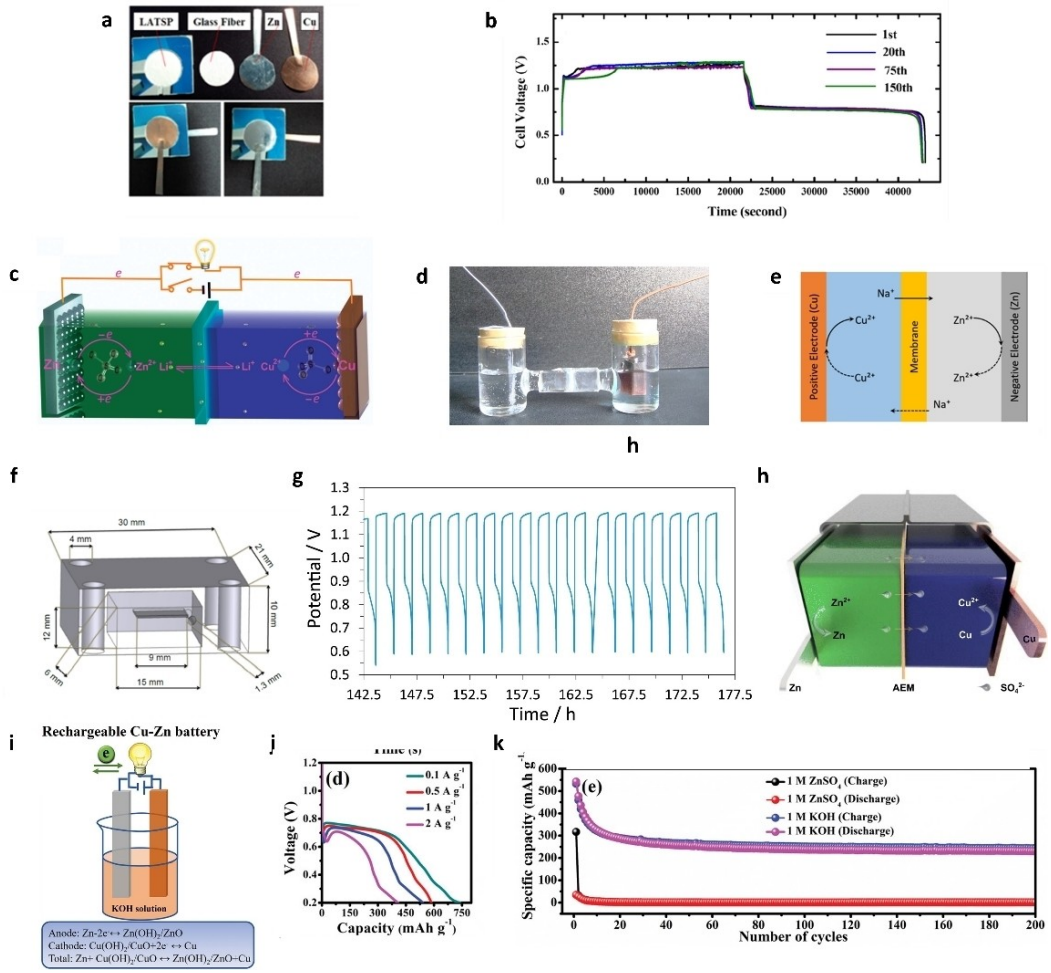

Figure 6. (a) Photographs of the LATSP-based Cu–Zn battery and (b) cyclic profile of the rechargeable Cu–Zn battery: cell voltage vs. time (re-print with permission from [21] Copyright 2014, Springer Nature); (c) schematic diagram of an aqueous rechargeable Cu–Zn Daniell type battery using Li^+ for charge transport; (d) the photograph of the Zn | $ZnSO_4 + Li_2SO_4$ | ion-block membrane | $CuSO_4 + Li_2SO_4$ | Carbon system (re-print with permission from [28] Copyright 2015, Royal Society of Chemistry); (e) schematic diagram of the rechargeable Cu–Zn battery using the CIMS membrane, (f) design of the battery testing device consisting of two identical components and (g) the voltage profile of the 80th to 100th cycle at 0.5 mA cm^{-2} with 0.1 M $CuSO_4$/1 M Na_2SO_4 on the cathode side and 1 M $ZnSO_4$ on the anode side (re-print with permission from [29] Copyright 2020, Elsevier); (h) schematic diagram of the Cu–Zn battery using AEM (re-print with permission from [30] Copyright 2023, Royal Society of Chemistry); (i) the rechargeable Cu–Zn battery with the alkaline electrolyte and (j) discharge curves of the Cu–Zn battery at 0.1, 0.5, 1, and 5 A g^{-1}; (k) the cycle performance of Cu–Zn battery in 1 M $ZnSO_4$ or 1 M KOH solution at the current rate of 1 A g^{-1} (re-print with permission from [31] Copyright 2019, Wiley-VCH)

The resulting alkaline Cu–Zn battery shows a high specific capacity of 718 mAh g^{-1} at 0.1 A g^{-1} with a discharge voltage of 0.76 V (Figure 6j). However, the battery experiences a fast capacity decay from 538 mAh g^{-1} in the first cycle to about 300 mAh g^{-1} after 20 cycles while cycling at 1 A g^{-1} (Figure 6k).

Even though the reversibility of aqueous Cu–Zn batteries has been significantly improved in recent publications, so far they all require the use of either two different electrolytes for the cathode and anode cells, which makes the battery difficult to be put into practical usage, or an alkaline solution that is harmful to both the environment and human health. Ideally, a single and benign electrolyte for both catholyte and anolyte would be desirable to simplify the structure of the Cu–Zn battery and make it more environmentally friendly. In addition, more investigations are needed to understand the interactions among the electrodes, electrolytes, and membranes to increase the long-terms stability of the battery.

3. Other Metal Cathodes

Apart from Cu, there are other metals with high electrode potential that can be used as the cathode in a battery, and they are summarized here.

3.1. Silver

One of the problems of a metal cathode is the migration of dissolved metal cations from the cathode to anode. This problem can be suppressed if the product is insoluble in the electrolyte. Amongst different metal compounds, AgCl is a well-known material with low solubility. As a demonstration, Wang et al. investigated the use of a Ag/AgCl redox reaction as the cathode of a battery. Lithium is used as the anode with 1 M $LiPF_6$ and 0.05 M LiCl in EC:DEC (diethyl carbonate) = 1 : 1

solution as the electrolyte.[32] As illustrated in Figure 7a, during the charge process, Ag is electrochemically oxidized, loses electrons, and becomes insoluble AgCl in the presence of Cl^- in the electrolyte solution. During the discharge process, a reversed reaction occurs, with AgCl electrochemically reduced to Ag. (Figure 7b) The charge/discharge reactions of the Ag cathode are shown below:

$$Ag - e^- + Cl^+ \leftrightarrow AgCl$$

Though, because the reaction involves the incorporation of Cl^- into Ag, a solid-state reaction, the available capacity depends strongly on the particle size and surface area of Ag, as shown in Figure 7c. Cathode with nano-particles Ag exhibits a higher specific capacity (about 70 mAh g^{-1}) than that of micron-sized Ag (about 10 mAh g^{-1}). Utilization of Ag can be further increased by growing nano-sized Ag particles on carbon nanotubes (n-Ag/CNT) (Figure 7d). The higher electrical conductivity of the electrode and smaller particle size can help facilitate the redox reaction of Ag/AgCl.

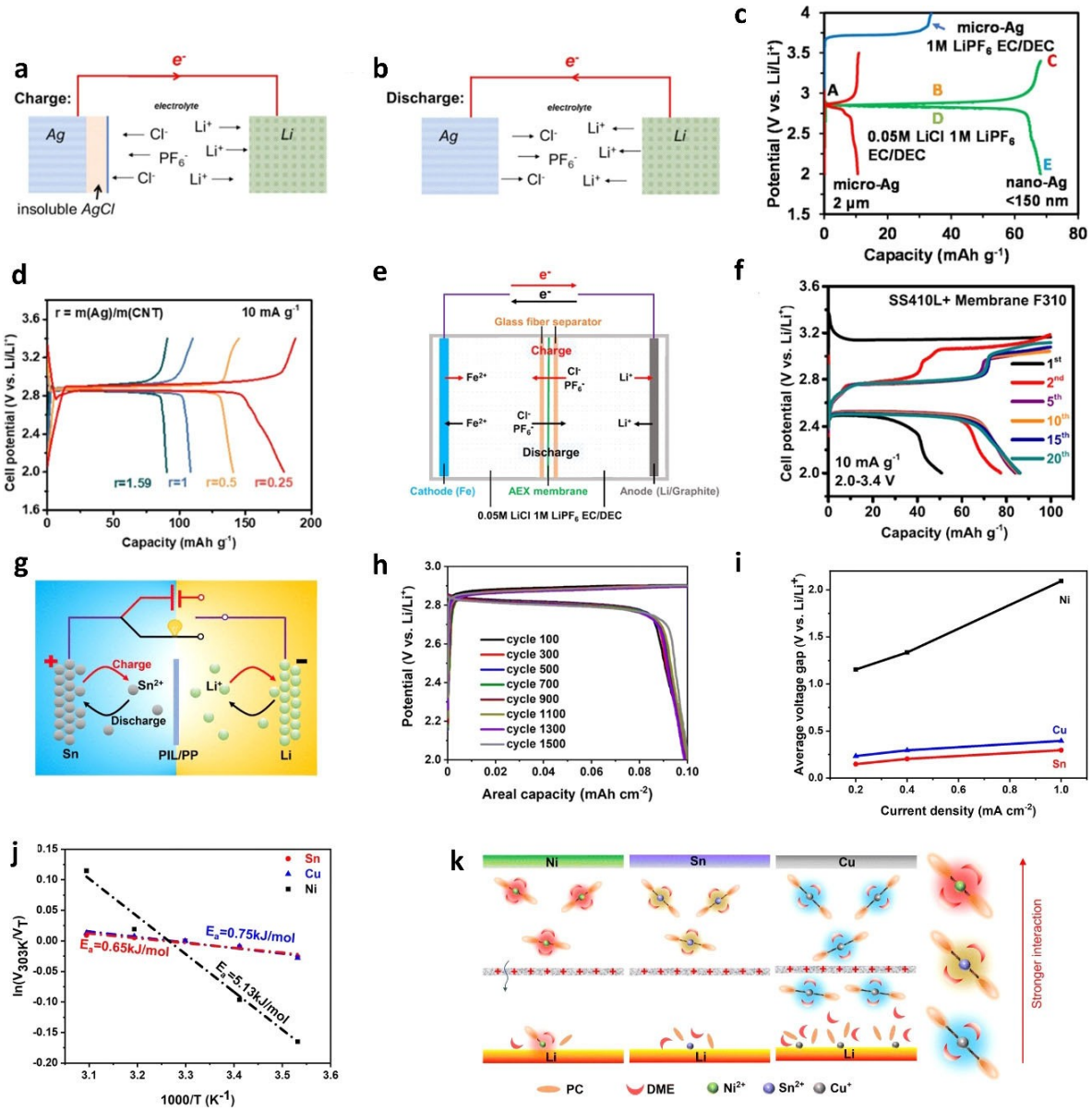

Figure 7. Schematic diagram of the Ag–Li system in the (a) charge process and (b) discharge process; (c) voltage profiles of micro- and nano-Ag powders; (d) charge-discharge profiles of Ag–CNT with different m(Ag)/m(CNT) ratios (re-print with permission from [32] Copyright 2019, Wiley-VCH); (e) schematic of the stainless-steel/lithium system; (f) voltage profiles of SS410 L half cells with F310 AEM membrane with a charge capacity limitation of 100 mAh g^{-1} at 10 mA g^{-1} (re-print with permission from [33] Copyright 2019, Elsevier); (g) schematic diagram of a Sn–Li battery; (h) selected charge/discharge curves of Sn–Li batteries at 0.2 mA cm^{-2} with an areal capacity limitation of 0.1 mA h cm^{-2}; (i) difference in polarization voltage of Sn–Li, Cu–Li, and Ni–Li batteries at different current densities; (j) Arrhenius plot of the average charge voltage (relative to values at 303 K) with respect to the battery temperature and (k) illustrations explaining the origin of the difference in the performance of different metal–lithium batteries (re-print with permission from [34] Copyright 2023, Royal Society of Chemistry).

The cycling stability of the n-Ag/CNT–Li battery in the 1 M $LiPF_6$ EC/DEC + LiCl electrolyte, however, is poor. This is attributed to the dissolution of AgCl into the electrolyte. Changing the electrolyte can enhance cycle stability, which suggests that the interaction between the electrolyte and the electrode material is critical for these types of batteries. Even though the utilization of an expensive noble metal, in this case Ag, is not practical, the study is an interesting demonstration of a metal conversion reaction for cathode applications and there could potentially be other similar reactions with more sustainable materials.

3.2. Iron/Stainless Steel

Fe is an inexpensive material that has a high electrode potential. Though, metallic Fe tends to be reactive to the environment, forming iron oxides spontaneously. To demonstrate the use of Fe as the cathode of a battery, Wang and Yu instead used stainless-steel powder with a large content of Fe as the starting material and developed a stainless-steel-Li battery, as shown in Figure 7e.[33] The solution of 1 M $LiPF_6$ + 0.05 M LiCl in EC:DEC = 1:1 was used as the electrolyte. Because stainless steel is rather inactive, LiCl is needed to facilitate the dissolution of Fe from it. During the charge process, the Fe atom in the stainless-steel cathode will lose two electrons, become Fe^{2+}, and dissolve into the electrolyte solution. Li^+ in the electrolyte solution will transform into Li and deposit on the anode surface. Reverse reactions will occur during the discharge process with Fe^{2+} deposited on the cathode surface and Li^+ released from the anode, respectively. To suppress the transfer of Fe^{2+} from the catholyte to the anolyte, the authors utilized a AEM (F310) in the cell, which effectively improved the CE to over 80% at a current rate of 10 mA g^{-1} (Figure 7f). Further work is needed to increase the CE by other strategies mentioned earlier in this review.

3.3. Tin

Xue et al. recently reported Sn foil as the cathode of a Sn–Li battery in a carbonate–ether based electrolyte with PC/DME (Figure 7g).[34] Using the PIL/PP AEM as the separator, the resulting Sn–Li battery gives a discharge voltage of about 2.8 V and can be cycled for more than 1500 times with an average CE of about 99.5% at a current density of 0.2 mA cm^{-2} with an areal capacity limitation of 0.1 mA h cm^{-2}, as shown in Figure 7h. The Sn–Li battery shows fast kinetics, with only a plateau voltage drop of 0.05 V even when the current rate is increased from 0.2 mA cm^{-2} to 1 mA cm^{-2} (corresponding to a current of 10 C).

Interestingly, the electrochemical performances of metal-Li batteries depend on the type of metals. Xue et al. compared the voltage polarization, activation energy, and CE of Sn, Cu, and Ni cathodes coupled with the Li anode under the same cell configuration, separator, and electrolyte and found that the redox reaction of Sn and Cu has lower activation energy (Figure 7i) and the voltage polarization is smaller than that of Ni ((Figure 7j). On the other hand, average CE of Sn and Ni is higher than that of Cu, suggesting that it is less likely for Sn^{2+} and Ni^{2+} to move through the PIL/PP membrane than Cu^+ (Figure 7k). Overall, Sn performs better than Cu and Ni as the cathode material using the PIL/PP membrane and the DME/PC-based electrolyte. Even though Sn has lower voltage than Cu and Ni, it could be a good cathode candidate considering kinetics and stability.

4. Liquid Metal batteries with Group IV, V, and VI Metals

Liquid metal battery (LMB) is another type of novel battery system using metals or alloys as the cathode, but requires a high working temperature (larger than 200 °C) to keep the cathode, anode and electrolyte in a liquid state.[35] As shown in Figure 8a, the liquid cathode, liquid anode, and liquid electrolyte are immiscible with each other, forming three distinctive layers due to the difference in densities. Lithium with lower density normally serves as the anode (top layer), while for the cathode side, metals from group IV, V, and VI with higher density (bottom layer) are typically adopted to form Li–Te, Li–Bi, Li–Sb, Li–Sn, and Li–Pb liquid metal batteries. The electrolyte is commonly a mixture of multiple molten halide salts such as LiCl–KCl, LiI–KI, LiCl–KCl–CsCl, etc. with a lower melting point than the single constitutes, which can act as both the electrolyte and separator. During the discharge process, the anode metal (Li) will be oxidized and release Li^+ into the molten salt electrolyte, which will then alloy with the cathode metal. A reversed process will take place during the charge process with the de-alloying of Li from the cathode, where the Li^+ will be transported through the electrolyte and reduced at the anode. Though, because the electrode potential for cathode metal-Li alloying is low, the nominal voltage of the battery is typically less than 1 V, as shown in Figure 8b.[36] Currently, the battery still experiences large voltage polarization with increasing current rates. In addition, the high-temperature working environment leads to higher energy consumption to maintain the metal electrodes and molten salt electrolytes in a liquid state and also limits the type of applications of such battery system.

5. Summary

The detailed information of all reviewed metal-cathode batteries are summarized in Table 2. In general, the charge transfer occurring in the batteries is originated from the redox reactions between metal and metal cations. Though, its performances are highly dependent on the type of the electrolyte, which will require more systematic investigations in the future. Cation crossover from the cathode side to the anode side is detrimental to the reversibility and long-term cycling stability of metal cathode batteries. Up to now, four strategies have been

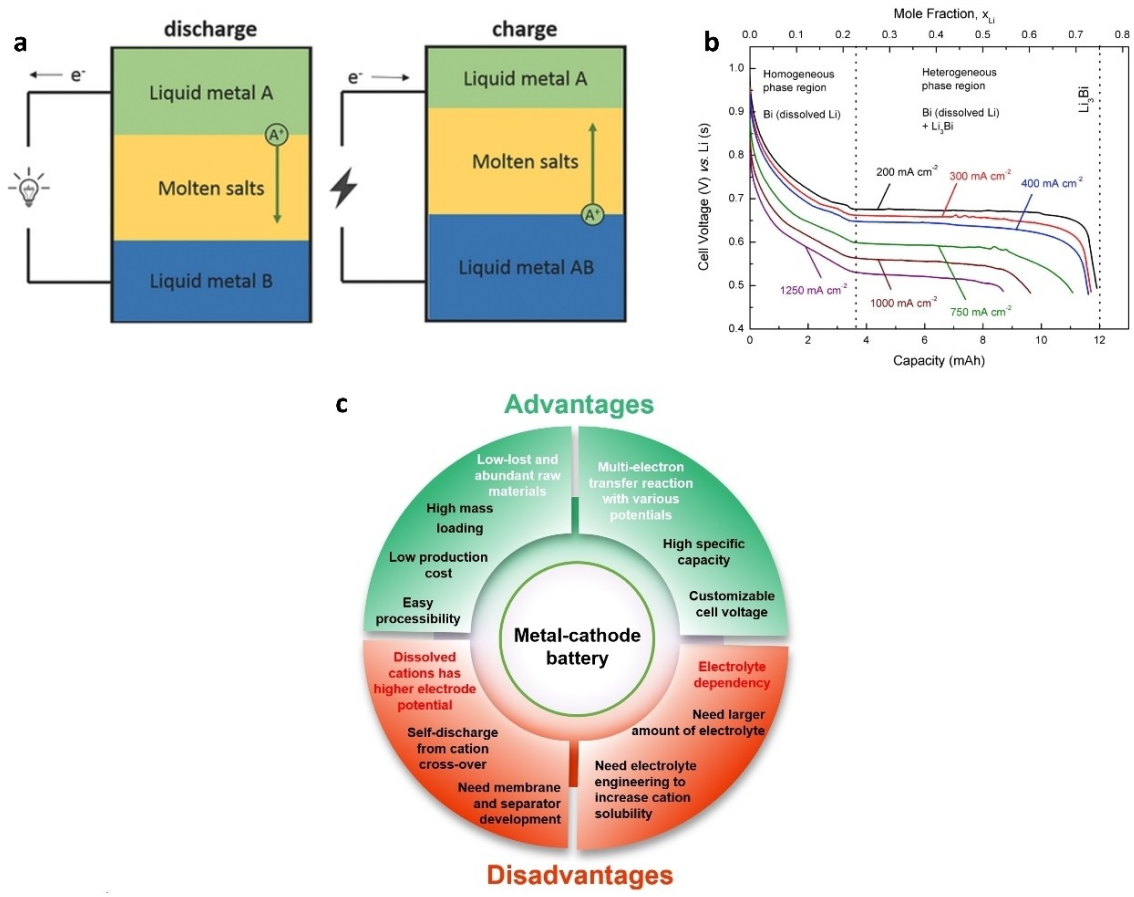

Figure 8. (a) Schematic diagram of the discharge and charge processes of a liquid metal battery (re-print with permission from [35] Copyright 2016, Wiley-VCH); (b) discharge curves of Li||LiCl–LiF||Bi liquid metal battery at T = 550 °C with different current densities(re-print with permission from [36] Copyright 2015, Elsevier); (c) advantages and disadvantages of the metal-cathode battery system.

proposed to solve the problem. The cycling stability of the battery is also affected by other factors such as the stripping/plating of the metal cathode.

The advantages of metal cathode batteries (Figure 8c) include (1) the low-cost and abundant raw materials; (2) the easy processibility of metal into foils which allows high mass loading and reduces production cost; (3) high specific capacities of the active materials as many metal cathodes can undergo a multi-electron transfer reactions and (4) customizable operating voltages by choosing metal cathodes and anodes with desirable electrode potentials. The disadvantages are (1) the dissolved cations are at a higher electrode potential than the anode, thus the cross-over of cations to the anode need to be prevented to reduce the self-discharge and electrode degradation, and (2) the large dependency of cell performance on electrolyte. In particular, a larger amount of electrolyte is needed to accommodate the cathode metal cations, which can limit the energy density of the battery. Regarding the disadvantages, future advances in the membrane or solid-state separator and the developments of the electrolyte with higher solubility are possible to overcome them.

6. Perspectives on Future Developments of Metal Cathodes

There are several crucial topics that need to be investigated to push the novel battery into practicability.

(a) Although the utilization of conductive metal foils as cathode increases the mass loading of active cathode materials and does away with the inactive current collector, right now, the areal capacity of the metal cathodes is still limited, typically lower than 0.1 mAh cm^{-2}, which means that the utilization rate of the metal cathode is rather low. There are currently some issues with the larger areal capacity. First, increasing areal capacity will typically lead to quicker failure of the battery due to the degradation/disintegration of the metal electrode. More studies to clarify the dissolution and deposition processes and also investigations on electrolyte additives and solvation structure of the electrolytes are needed to enable uniform stripping and plating of the metal to prolong cycle life. Second, the metal cations that are stripped from the cathode need to be stored in the catholyte, so larger areal capacity means larger amount of electrolyte is needed. In particular, organic electrolytes tend to have lower metal ions solubility than aqueous electrolytes, so the higher cell voltage when coupled with a metal anode with low electrode potential such as Li is negated

Table 2. A summary of different metal cathode batteries.

Battery	Cathode	Anode	Separator	Electrolyte	Capacity	Voltage (V)	Current (mA)	Coulombic efficiency	Ref.
Cu–Li	Cu powder	Li disc	DES gel/ LATP/ DES-FEC gel	DES gel/LATP/DES-FEC gel	500 mAh g^{-1}	2.75 and 4	200 mA g^{-1}	99.6%	[15]
Cu–Li	Au–Cu@CNFs	Li foil	C-coated separator	1.0 M $LiClO_4$ in EC/PC	755 mAh g^{-1}	3.5	200 mA g^{-1}	99%	[16]
Cu–Al	Cu foil	Al foil	AEM F310	6 M LiTFSI DMC	0.225 mAh cm^{-2}	3	0.0225 mA cm^{-2}	88%	[17]
Cu–Li	Cu foil	Li foil	PAA(BTO)/ PP	3 M LiTFSI DMC	0.1 mAh cm^{-2}	3.3	0.01 mA cm^{-2}	86%	[19]
Cu–Al	Cu foil	Al foil	PP	3 M LiTFSI FEC	0.14 mAh cm^{-2}	3	0.014 mA cm^{-2}	97%	[20]
Cu–Zn	Cu plate	Zn plate	LATSP film	2 M $LiNO_3$ water and 1 M $Zn(NO_3)_2$ water	1.5 mAh cm^{-2}	0.8	0.25 mA cm^{-2}	98%	[21]
Cu–Al	Cu/PAN	Al foil	PP	3 M LiTFSI FEC	0.14 vmAh cm^{-2}	3	0.014 mA cm^{-2}	98%	[22]
Cu–Li	Cu foil	Li foil	PIL/PP	3 M LiTFSI DMC	0.1 vmAh cm^{-2}	3.3	0.2 mA cm^{-2}	99%	[24]
Cu–Li	Cu foil	Li foil	LISICON film	1 M $LiClO_4$ EC/DMC and 2 M $LiNO_3$ water	16 mAh cm^{-2}	3.1	1 mA cm^{-2}	99%	[25]
Cu–Li	Cu foil	Li foil	PIL/PP	3 M LiTFSI DME/PC	0.1 mAh cm^{-2}	3.3	2 mA cm^{-2}	99%	[27]
Cu–Zn	Cu plate	Zn plate	PVDF/ PMMA-Li-ClO_4/ PVDF	0.1 M $CuSO_4$/1 M Li_2SO_4 water and 0.1 M $ZnSO_4$/1 M Li_2SO_4 water	330 mA h g^{-1}	0.96	1 mA cm^{-2}	100%	[28]
Cu–Zn	Cu plate	Zn plate	CIMS	0.1 M $CuSO_4$/1 M Na_2SO_4 water and 1 M $ZnSO_4$ water	763 mAh g^{-1}	0.8	0.5 mA cm^{-2}	100%	[29]
Cu–Zn	Cu foil	Zn foil	AEM FAA-3- PK-130	1.0 M $CuSO_4$/H_2SO_4 water and 2 M $ZnSO_4$ water	10 mAh cm^{-2}	0.86	10 mA cm^{-2}	100%	[30]
Cu–Zn	Cu clusters	Zn foil	NKK	1 M KOH water	718 mAh g^{-1}	0.76	0.1 A g^{-1}	100%	[31]
Ag–Li	nano-Ag/CNT	Li foil	glass fiber	1 M $LiPF_6$/0.05 M LiCl EC/DEC	180 mAh g^{-1}	2.8	10 mA g^{-1}	95%	[32]
Fe–Li	Stainless-steel powder	Li foil	AEM F310	1 M $LiPF_6$/0.05 M LiCl EC/DEC	100 mAh g^{-1}	2.5	10 mA g^{-1}	90%	[33]
Sn–Li	Sn foil	Li foil	PIL/PP	3 M LiTFSI DME/PC	0.1 mA h cm^{-2}	2.8	0.2 mA cm^{-2}	99.5%	[34]
Li–Bi	Liquid Bi	Liquid Li	LiCl-LiF molted salt	LiCl-LiF molted salt	3.33 mAh cm^{-2}	0.68	200 mA cm^{-2}	100%	[36]

by the lower solubility of the electrolyte. Thus, the practical energy density of the battery with metal cathode is expected to be lower than that of LIBs, but can be comparable or even exceed that of redox flow batteries with further optimizations. Further work on exploring electrolytes with higher solvating ability towards metal cations are essential for the future development for metal cathode battery systems.

(b) Further works are needed to improve the CE of the batteries with metal cathode to stop the cross-over of metal cations from the catholyte to the anolyte. Currently, solid electrolyte separators tend to have poor kinetics, while polymer membranes cannot achieve CE of 100%. More effective separators and electrolytes are desired to reduce the self-discharge of the batteries.

(c) Aside from problems related to the metal cathodes, there are also significant issues such as dendrite formation and gas generation if it is coupled with another metal anode such as Li or Zn. At the end, strategies that can be compatible with both the metal cathode and anode are required for full cell operations in the future.

Acknowledgements

This study was supported by a Research Matching Grant Scheme (PJ9229008) by the government of Hong Kong Special Administrative Region.

Conflict of Interests

The authors declare no conflict of interest.

Data Availability Statement

The data that support the findings of this study are available from the corresponding author upon reasonable request.

Keywords: Cation crossover · dissolution/deposition · electrolyte · membrane · metal cathode

[1] Y. Liang, C.-Z. Zhao, H. Yuan, Y. Chen, W. Zhang, J.-Q. Huang, D. Yu, Y. Liu, M.-M. Titirici, Y.-L. Chueh, H. Yu, Q. Zhang, *InfoMat.* **2019**, *1*, 6–32.
[2] B. Dunn, H. Kamath, J.-M. Tarascon, *Science* **2011**, *334*, 928–935.
[3] J. Deng, C. Bae, A. Denlinger, T. Miller, *Joule* **2020**, *4*, 511–515.
[4] M. Li, J. Lu, Z. Chen, K. Amine *Adv. Mater.* **2018**, *30*, 1800561.
[5] G. Patry, A. Romagny, S. Martinet, D. Froelich, *Energy Sci. and Eng.* **2015**, *3*, 71–82.
[6] W.-J. Kwak, Rosy, D. Sharon, C. Xia, H. Kim, L. R. Johnson, P. G. Bruce, L. F. Nazar, Y.-K. Sun, A. A. Frimer, M. Noked, S. A. Freunberger, D. Aurbach, *Chem. Rev.* **2020**, *120*, 6626–6683.
[7] G. Zhou, H. Chen, Y. Cui, *Nat. Energy* **2022**, *7*, 312–319.
[8] X. Wu, A. Markir, L. Ma, Y. Xu, H. Jiang, D. P. Leonard, W. Shin, T. Wu, J. Lu, X. Ji, *Angew. Chem. Int. Ed.* **2019**, *58*, 12640–12645.
[9] M. Yu, Y. Sui, S. K. Sandstrom, C.-Y. Wu, H. Yang, W. Stickle, W. Luo, X. Ji, *Angew. Chem. Int. Ed.* **2022**, *61*, e202212191.
[10] C. Xu, C. Lei, J. Li, X. He, P. Jiang, H. Wang, T. Liu, X. Liang, *Nat. Commun.* **2023**, *14*, 2349.
[11] Y. Ding, X. Guo, Y. Qian, L. Xue, A. Dolocan, G. Yu, *Adv. Mater.* **2020**, *32*, 2002577.
[12] M. Wang, F. Zhang, C.-S. Lee, Y. Tang, *Adv. Energy Mater.* **2017**, *7*, 1700536.
[13] J. Shin, J. Lee, Y. Park, J. W. Choi, *Chem. Sci.* **2020**, *11*, 2028–2044.
[14] X. Wu, A. Markir, Y. Xu, C. Zhang, D. P. Leonard, W. Shin, X. Ji, *Adv. Funct. Mater.* **2019**, *29*, 1900911.
[15] H. Wang, C. Wang, M. Zheng, J. Liang, M. Yang, X. Feng, X. Ren, D. Y. W. Yu, Y. Li, X. Sun, *Angew. Chem. Int. Ed.* **2023**, *62*, e202214117.
[16] Y. Huang, W. Zhang, S. Li, W. Luo, Z. Huang, C. Fang, M. Weng, J. Zheng, F. Pan, Q. Liu, Y. Huang, *Nano Energy* **2018**, *54*, 59–65.
[17] H. Wang, D. Y. W. Yu, *ACS Appl. Energ. Mater.* **2019**, *2*, 4936–4942.
[18] M. F. Lagadec, R. Zahn, V. Wood, *Nat. Energy* **2019**, *4*, 16–25.
[19] K. Xue, H. Wang, P.-K. Lee, S. Dong, D. Y. W. Yu, *ACS Appl. Mater. Interfaces* **2021**, *13*, 47449–47457.
[20] H. Wang, Y. Sun, M. Li, G. Li, K. Xue, Z. Chen, D. Y. W. Yu, *Small* **2020**, *16*, 2003438.
[21] X. Dong, Y. Wang, Y. Xia, *Sci. Rep.* **2014**, *4*, 6916.
[22] H. Wang, K. Xue, B. Su, D. Y. W. Yu, *Electrochim. Acta* **2021**, *388*, 138595.
[23] M. A. Hickner, A. M. Herring, E. B. Coughlin, *J. Polym. Sci. B Polym. Phys.* **2013**, *51*, 1727–1735.
[24] K. Xue, Y. Zhao, P.-K. Lee, D. Y. W. Yu, *Energy Environ.* **2023**, *6*, e12395.
[25] Y. Wang, H. Zhou, *Electrochem. Commun.* **2009**, *11*, 1834–1837.
[26] H. Zhou, Y. Wang, H. Li, P. He, *ChemSusChem.* **2010**, *3*, 1009–1019.
[27] K. Xue, Y. Zhao, H. Wang, D. Y. W. Yu, *J. Energy Chem.* **2023**, *86*, 208–216.
[28] H. Zhang, T. Yang, X. Wu, Y. Zhou, C. Yang, T. Zhu, R. Dong, *Chem. Commun.* **2015**, *51*, 7294–7297.
[29] A. Jameson, A. Khazaeli, D. P. J. Barz, *J. Power Sources* **2020**, *453*, 227873.
[30] Z. He, J. Guo, F. Xiong, S. Tan, Y. Yang, R. Cao, G. Thompson, Q. An, M. De Volder, L. Mai, *Energy Environ. Sci.* **2023**, *16*, 5832–5841.
[31] Q. Zhu, M. Cheng, B. Zhang, K. Jin, S. Chen, Z. Ren, Y. Yu, *Adv. Funct. Mater.* **2019**, *29*, 1905979.
[32] H. Wang, W. Gu, D. Y. W. Yu, *ChemElectroChem.* **2019**, *6*, 3627–3632.
[33] H. Wang, D. Y. W. Yu, *Electrochim. Acta* **2019**, *298*, 186–193.
[34] K. Xue, Y. Zhao, P.-K. Lee, D. Y. W. Yu, *J. Mater. Chem. A* **2023**, *11*, 1482–1490.
[35] H. Li, H. Yin, K. Wang, S. Cheng, K. Jiang, D. R. Sadoway, *Adv. Energy Mater.* **2016**, *6*, 1600483.
[36] X. Ning, S. Phadke, B. Chung, H. Yin, P. Burke, D. R. Sadoway, *J. Power Sources* **2015**, *275*, 370–376.

Manuscript received: November 11, 2023
Revised manuscript received: December 27, 2023
Version of record online: ■■, ■■

REVIEW

Metal-cathode battery is a novel battery system where low-cost, abundant metals with high electrode potential can be used as the positive electrode material. Recent progresses with emphases on the cathode, anode, electrolyte, and separator of the batteries are summarized and future research directions are proposed in this review paper.

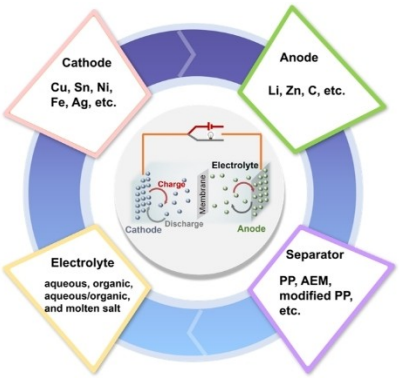

*Dr. K. Xue, Dr. H. Wang, Prof. D. Y. W. Yu**

1 – 16

Emerging Battery Systems with Metal as Active Cathode Material